$E2$ transition and Q_{J^+} systematics of even mass xenon nuclei

Rani Devi, S. P. Sarswat, Arun Bharti, and S. K. Khosa
Department of Physics, Jammu University, Jammu, 180004, India
(Received 31 July 1996; revised manuscript received 13 January 1997)

The yrast spectra with $J^{\pi}_{\max}=10^{+}$, $B(E2)$ transition probabilities and Q_{J^+} values are calculated for even-even xenon isotopes by carrying out variation-after-projection calculations in conjunction with a Hartree-Fock-Bogoliubov (HFB) ansatz employing a pairing-plus-quadrupole-quadrupole effective interaction operating in a reasonably large valence space outside the ^{100}Sn core. Our calculations reveal that the systematics of low-lying yrast states in these isotopes are intricately linked with the manner in which neutrons tend to occupy the various valence orbits. The results on $B(E2)$ transition probabilities predict a dip in the isotopes ^{114,116,120,124,128}Xe, which might be construed to imply different structures for ^{114,116,120,124,128}Xe as compared to their neighbors. Besides this, our results also reveal that both the HFB technique and the quadrupole-quadrupole-plus-pairing model of the two-body interaction are fairly reliable in this mass region. [S0556-2813(97)04604-9]

PACS number(s): 21.10.Ky, 21.60.Jz, 27.60.+j

I. INTRODUCTION

The ground state properties of even-even Xe isotopes have been the subject of experimental studies [1–9] involving in-beam γ-ray spectroscopy. The principal features of the nuclear structure of these nuclides appear to vary smoothly over a large range of neutron number. With four protons beyond the closed shell at $Z=50$, these nuclides are too complex for shell model calculations without the severest approximations and yet not so deformed as to be considered among the classical prolate rotors such as ^{168}Er.

An interesting feature of the observed yrast spectra is the systematic variation of $E_{2_1^+}$, $E_{4_1^+}$, $E_{6_1^+}$ excitation energy from ^{114}Xe to ^{130}Xe. It is observed that these states approximately follow a parabolic type of systematics with a minimum energy for these states occurring at ^{122}Xe. It is believed that the investigation of the level structure of the even-even Xe nuclides can yield important information regarding the collective properties of nuclides which cannot be clearly classified as either rotational or vibrational.

The level properties of Xe nuclei have been described by a number of methods ranging from a simple variable moment of inertia approach, in which only the yrast band is considered, to more complex approaches involving collective excitation. Among several approaches to the description of the collective states of even-even Xe nuclei, there are some which tend to derive the collective properties of nuclei in a microscopic way.

The results of a number of such calculations are available for Xe nuclei. For example, one has been performed by Rohozinski *et al.* [10], and the other by Otsuka *et al.* [11]. In the first approach the dynamic calculations have been carried out using the collective quadrupole Bohr Hamiltonian, where the potential energy and the six inertial functions are obtained microscopically. In the second approach the shell model interpretation of the interacting bosons in the interacting boson model (IBM) model provides the microscopic description of the collective states. The results of both models obtained with the microscopic input and without free parameters, although reflecting general trends, are not in good agreement with experimental data. It was shown that a reduction of the pairing interaction strength in the approach of Rohozinski *et al.* [10] and the renormalization of the boson energies in the IBM improve remarkably the agreement with experiment. Recently, Mantica *et al.* [9] have carried out IBM2 calculations for a set of nuclei $^{124-128}$Xe. These calculations are distinguished from previous efforts as they hold many of the parameters constant and permit only slow variations in the others. These fits have been made completely with the IBM2 without recourse to the introduction of either triaxiality or particle intruder hole structures. The calculations support the notion that these Xe nuclides are moderately deformed at low energy and that deviation from symmetry only develops at higher rotational frequency.

From the overview of the theoretical work, it is evident that there is no single microscopic framework that has been applied uniformly to the entire set of neutron-rich Xe isotopes with a single set of input parameters. It is with this motivation in mind we plan to carry out a study of low-lying yrast spectra in the entire set of Xe isotopic mass chains in a suitable microscopic framework. The basic elements of such a calculational framework, such as the choice of core, the valence space, and two-body residual interaction, have, however, to be made very judiciously. One of the guiding principles for making this choice is that the quadrupole moments of the intrinsic states as a function of neutron number should exhibit a trend similar to that implied by experimental $E2$ transition rates. The deformed Hartree-Fock-Bogoliubov (HFB) state of the nucleus generated by the effective interaction provides a reasonable intrinsic state of the nucleus. Therefore the goodness of the effective interaction and completeness of the valence space can be checked by finding whether it generates intrinsic states whose quadrupole moments exhibit a trend similar to that implied by experimental $E2$ transition rates.

In this paper, we carry out a microscopic study of the yrast states, $B(E2)$ transition probabilities, and Q_{J^+} values in the nuclei $^{114-130}$Xe, by employing the variation after pro-

jection (VAP) [12] formalism in conjunction with the HFB [13] ansatz for the axially symmetric intrinsic wave functions.

In the present variational calculation of the yrast levels in the nuclei $^{114-130}$Xe, we have employed the usual pairing-plus-quadrupole-quadrupole effective interaction operating in a valence space spanned by the $3s_{1/2}$, $2d_{3/2}$, $2d_{5/2}$, $2f_{7/2}$, $1g_{7/2}$, $1h_{9/2}$, and $1h_{11/2}$ orbits for protons as well as neutrons. The nucleus ^{100}Sn has been considered as a core.

II. CALCULATIONAL DETAILS

A. One- and two-body parts of the Hamiltonian

The spherical single-particle energies (SPE's) that are employed here are (in MeV) $(2d_{5/2})=0.0$, $(3s_{1/2})=1.4$, $(2d_{3/2})=2.0$, $(1g_{7/2})=4.0$, $(1h_{11/2})=6.5$, $(2f_{7/2})=12.0$, and $(1h_{9/2})=12.5$. This set of input SPE's for the states $2d_{5/2}$, $3s_{1/2}$, $2d_{3/2}$, $1g_{7/2}$, and $1h_{11/2}$ are nearly the same as that employed by Vergados and Kuo [14] as well as Federman *et al.* [15] except that the energy of $1h_{11/2}$ has been increased by about 1.5 MeV. The energy gap between the $2f_{7/2}$ and $1h_{11/2}$ orbits was calculated to be about $0.45\hbar\omega$ from the Nilsson diagram, published in the book by Pal [16]. By taking $\hbar\omega\approx 8.5$ MeV [17] in this mass region, the energy gap works out to be 3.82 MeV. The energy gap used by us is 5.5 MeV. This gap between the energy states had to be increased to reproduce shell closure for $N=82$ as observed in ^{134}Te. In the case where this gap is reduced, the calculations reveal that ^{134}Te is quasideformed, which is contrary to what is observed experimentally. Therefore the SPE's of $1h_{11/2}$, $2f_{7/2}$, and $1h_{9/2}$ orbits were adjusted to reproduce shell closures for $N=82$ for ^{134}Te.

The two-body effective interaction that has been employed is of ''pairing-plus-quadrupole-quadrupole $(q\text{-}q)$'' type [18]. The pairing part can be written as

$$V_P=-(G/4)\sum_{\alpha\beta} S_\alpha S_\beta a^\dagger_\alpha a^\dagger_{\bar{\alpha}} a_{\bar{\beta}} a_\beta, \tag{1}$$

where α denotes the quantum numbers $(nljm)$. The state $\bar{\alpha}$ is the same as α, but with the sign of m reversed. Here S_α is the phase factor $(-1)^{j-m}$. The $q\text{-}q$ part of the two-body interaction is given by

$$V_{qq}=-(\chi/2)\sum_{\alpha\beta\gamma\delta}\sum_{\mu}\langle\alpha|q^2_\mu|\gamma\rangle\langle\beta|q^2_{-\mu}|\delta\rangle \times(-1)^\mu a^\dagger_\alpha a^\dagger_\beta a_\delta a_\gamma, \tag{2}$$

where the operator q^2_μ is given by

$$q^2_\mu=(16\pi/5)^{1/2} r^2 Y^2_\mu(\Theta,\Phi). \tag{3}$$

The strengths for the like-particle neutron-neutron $(n\text{-}n)$, proton-proton $(p\text{-}p)$, and neutron-proton $(n\text{-}p)$ components of the quadrupole-quadrupole $(q\text{-}q)$ interaction were taken as

$$\chi_{nn}(=\chi_{pp})=-0.0122 \text{ MeV b}^{-4},$$

$$\chi_{np}=-0.0230 \text{ MeV b}^{-4}.$$

Here b $(=\sqrt{\hbar/m\omega})$ is the oscillator parameter. These values for the strengths of the $q\text{-}q$ interactions compare favorably with the ones suggested by Arima [19] and are very near to the ones employed in earlier study of deformation systematics in the $A\simeq 100$ region by Khosa *et al.* [20]. The strength for the pairing interaction was fixed through the approximate relation $G=18-21/A$) at $G=-0.20$ MeV.

B. Projection of states of good angular momentum from axially symmetric HFB intrinsic states

The assumption concerning the axial symmetry of the intrinsic states is consistent with the microscopic calculation of the potential energy surfaces in ^{102}Zr by Kumar *et al.* [21]. It is found that the minimum of potential energy $V(\beta,\gamma)$ for the ground state band occurs at $\beta=0.4$ and $\gamma=10°$ and, therefore, the effects due to nonaxiality are expected to be small for the yrast levels for nuclei with $A\approx 100$. In what follows we give a brief outline of the method of projecting out the eigenstates of $\hat{J}^2$ from the axially symmetric intrinsic states.

The axially symmetric intrinsic HFB state with $k=\langle\hat{J}_z\rangle=0$ can be written as

$$|\Phi_0\rangle=\prod_{im}(U^m_i+V^m_i b^\dagger_{im} b^\dagger_{\bar{im}})|0\rangle, \tag{4}$$

where the creation operator $b^\dagger_{im}$ can be expressed as

$$b^\dagger_{im}=\sum_j C^m_{ji} a^\dagger_{jm}, \quad b^\dagger_{\bar{im}}=\sum_j (-1)^{j-m} C^m_{ji} a^\dagger_{j-m}. \tag{5}$$

Here the index i labels the different orbitals with the same $\langle\hat{J}_z\rangle=m$ and j labels the spherical single-particle states of the valence space.

The states with good angular momenta J projected from the HFB state $|\Phi_k\rangle$ can be written as

$$|\psi^J_k\rangle=P^J_{kk}|\Phi_k\rangle=(2J+1)/8\pi^2\int D^J_{kk}(\Omega)R(\Omega)|\Phi_k\rangle d\Omega, \tag{6}$$

where $R(\Omega)$ and $D^J_{kk}(\Omega)$ are the rotational operator and the rotation matrix, respectively.

The energy of a state with angular momentum J is given as

$$E_J=\langle\Phi_0|HP^J_{00}|\Phi_0\rangle/\langle\Phi_0|P^J_{00}|\Phi_0\rangle = \frac{\int_0^\pi h(\theta)d^J_{00}(\theta)d(\cos\theta)}{\int_0^\pi n(\theta)d^J_{00}(\theta)d(\cos\theta)}. \tag{7}$$

Here the overlap integrals $h(\theta)$ and $n(\theta)$ are given by

$$h(\theta)=n(\theta)\Bigg[\sum_{\alpha}\ \epsilon(\alpha)\rho_{\alpha\alpha}-(G/4)\sum_{\tau_3\alpha}\ S_{\alpha}\{f(1+M)^{-1}\}^{\tau_3}_{\alpha\alpha}$$

$$\times\sum_{\beta}\ S_{\beta}\{(1+M)^{-1}F\}^{\tau_3}_{\beta\beta}-\frac{1}{2}\sum_{\tau_3\tau_3'\mu}\ (-1)^{\mu}\kappa_{\tau_3\tau_3'}$$

$$\times\sum_{\alpha\gamma}\ \langle\alpha|q^2_{\mu}|\gamma\rangle\rho^{\tau_3}_{\gamma\alpha}\sum_{\beta\delta}\ \langle\beta|q^2_{-\mu}|\delta\rangle\rho^{\tau_3'}_{\delta\beta}\Bigg], \tag{8}$$

$$n(\theta)=\{\det[1+M(\theta)]\}^{1/2}, \tag{9}$$

where

$$F_{\alpha\beta}(\theta)=\sum_{m'_{\alpha}m'_{\beta}}\ d^{j_{\alpha}}_{m_{\alpha}m'_{\alpha}}(\theta)d^{j_{\beta}}_{m_{\beta}m'_{\beta}}(\theta)f_{j_{\alpha}m'_{\alpha},j_{\beta}m'_{\beta}}, \tag{10}$$

$$f_{\alpha\beta}=\sum_{i}\ C^{m_{\alpha}}_{j_{\alpha}i}C^{m_{\beta}}_{j_{\beta}i}\left(\frac{V^m_i\alpha}{U^m_i\alpha}\right)\delta_{m_{\alpha},-m_{\beta}}, \tag{11}$$

$$M=Ff^{\dagger},\quad \rho(\theta)=M(\theta)/[1+M(\theta)]. \tag{12}$$

The yrast energies are calculated as follows. Using the results of the HFB calculations—and these are summarized in terms of amplitudes (U^m_i, V^m_i) and the expansion coefficients C^m_{ij}—we first set up the (50×50) f matrix in the present valence space. Then F, M, and $(I+M)^{-1}$ are computed for 20 Gaussian quadrature points in the range $(0,\pi/2)$. Finally, the projected energies are calculated employing Eqs. (7)–(9).

It may be mentioned that variational methods quite similar to the ones employed here have been used earlier by Faessler, Lin, and Wittman [22] as well as by Nair and Ansari [23] in connection with the study of backbending effects in ^{158}Er. The present calculation, however, employs exact angular momentum projection in contrast with the technique used by Nair and Ansari which used an approximation suggested by Das Gupta and Van Ginneken [24].

C. Variation-after-angular-momentum projection method

The calculation of the energies of the yrast levels has been carried out as follows: First, the self-consistent axially symmetric HFB solutions $\Phi_{k=0}(\beta)$, resulting from the Hamiltonian $(H-\beta Q^2_0)$, where β is a parameter, are generated. The optimum intrinsic state for each J, $\Phi_{\rm opt}(\beta_J)$, has been selected by determining minimum of the projected energy,

$$E_J(\beta)=\langle\Phi(\beta)|HP^J_{00}|\Phi(\beta)\rangle/\langle\Phi(\beta)|P^J_{00}|\Phi(\beta)\rangle, \tag{13}$$

as a function of β. In other words, the optimum intrinsic state for each yrast J satisfies the condition

$$\partial/\partial\beta[\langle\Phi(\beta)|HP^J_{00}|\Phi(\beta)\rangle/\langle\Phi(\beta)|P^J_{00}|\Phi(\beta)\rangle]=0. \tag{14}$$

D. Electric quadrupole transition matrix element for the yrast states

The matrix elements of the quadrupole operator between the yrast states belonging to different intrinsic states can be given as

$$\langle\psi^{J'}_K(\beta')|Q^2_0|\psi^J_K(\beta)\rangle$$

$$=[n^J(\beta)n^{J'}(\beta')]^{-1/2}\int_0^{\pi/2}\sum_{\mu}\begin{bmatrix} J & 2 & J' \\ -\mu & \mu & 0\end{bmatrix}d^J_{\mu0}(\theta)n(\beta,\beta',\theta)b^2\Bigg[\sum_{\tau_3\alpha\beta}\ e_{\tau_3}\langle\alpha|Q^2_{\mu}|\beta\rangle\rho^{\tau_3}_{\alpha\beta}(\beta,\beta',\theta)\Bigg]\sin\ \theta\ d\theta, \tag{15}$$

where

$$n^J(\beta)=\int_0^{\pi}[\det\{1+F(\beta,\theta)f^{\dagger}(\beta,\theta)\}]^{1/2}d^J_{00}(\theta)\sin\ \theta\ d\theta, \tag{16}$$

$$n(\beta,\beta',\theta)=(\det\{[1+F(\beta,\theta)]f^{\dagger}(\beta',\theta)\})^{1/2}, \tag{17}$$

and

$$\rho^{\tau_3}_{\alpha\beta}(\beta,\beta',\theta)=\{M(\beta,\beta',\theta)/[1+M(\beta,\beta',\theta)]\}^{\tau_3}_{\alpha\beta}, \tag{18}$$

with

$$M(\beta,\beta',\theta)=F(\beta,\theta)f^{\dagger}(\beta',\theta).$$

TABLE I. Experimental values of excitation energy of the E_{2^+} state (ΔE), intrisic quadrupole moments of the HFB states in some doubly even Xe isotopes. Here $\langle Q^2_0\rangle_{\pi}$ ($\langle Q^2_0\rangle_{\nu}$) gives the contribution of the protons (neutrons) to the total intrinsic quadrupole moment. The quadrupole moments have been computed in units of b^2, where b $(=\sqrt{\hbar/m\omega})$ is the harmonic oscillator parameter.

Xenon nuclei	E_{2^+} (MeV)	$\langle Q^2_0\rangle_{\rm HFB}$	$\langle Q^2_0\rangle_{\pi}$	$\langle Q^2_0\rangle_{\nu}$
114	0.45	49.70	20.00	29.70
116	0.39	59.47	20.90	38.57
118	0.34	67.24	21.36	45.88
120	0.32	69.48	21.46	48.02
122	0.33	76.75	22.16	54.59
124	0.35	71.01	21.70	49.31
126	0.39	64.21	21.50	42.72
128	0.44	58.41	20.81	37.60
130	0.54	54.82	20.57	34.25

TABLE II. Subshell occupation numbers (neutrons) in the nuclei $^{114-130}$Xe and ^{134}Te showing shell closure at $N=82$.

Xenon nuclei (A)	Subshell occupation number						
	$3s_{1/2}$	$2d_{3/2}$	$2d_{5/2}$	$2f_{7/2}$	$1g_{9/2}$	$1h_{9/2}$	$1h_{11/2}$
^{114}Xe	0.79	1.84	4.30	0.14	2.07	0.02	0.85
^{116}Xe	0.86	1.87	4.28	0.39	2.50	0.03	2.01
^{118}Xe	0.94	1.89	4.42	0.64	3.03	0.03	3.05
^{120}Xe	1.08	1.95	5.06	0.75	3.57	0.03	3.56
^{122}Xe	1.08	1.95	5.12	0.99	3.85	0.06	4.95
^{124}Xe	1.24	2.11	5.61	0.95	4.81	0.08	5.21
^{126}Xe	1.65	2.81	5.78	0.89	5.26	0.10	5.52
^{128}Xe	1.87	3.47	5.91	0.85	5.80	0.10	5.99
^{130}Xe	1.98	3.89	5.98	0.82	6.34	0.09	6.89
^{134}Te	2.00	4.00	6.00	0.23	8.00	0.10	11.75

III. RESULTS OF HFB AND VAP CALCULATIONS ON Xe ISOTOPES

A. Deformation systematics of Xe isotopes

It is well known from Grodzins's rule [25] that E_{2^+} systematics bear an inverse correlation to the observed Q_{2^+} systematics. Since Q_{2^+} of a nucleus is directly related to its intrinsic quadrupole moment, the observed systematics of E_{2^+} with A should produce a corresponding inverse systematics of intrinsic quadrupole moments of Xe nuclei with increasing A. Based upon the above logic, the calculated values of intrinsic quadrupole moments should exhibit a systematic increase as we go from ^{114}Xe to ^{122}Xe. Thereafter, for the set of $^{124-130}$Xe nuclei, the intrinsic quadrupole moments should show a decreasing trend. In Table I the results of HFB calculations are presented. Note that the intrinsic quadrupole moments systematically increase for the set of $^{114-122}$Xe isotopes. Thereafter the intrinsic quadrupole moments systematically show a downward trend. For example, the $\langle Q_0^2 \rangle$ value for ^{114}Xe is 49.7 units and that for ^{122}Xe is 76.7 units. Besides this, the $\langle Q_0^2 \rangle$ value is 54.82 units for ^{130}Xe. Thus the calculated values of $\langle Q_0^2 \rangle$ reproduce qualitatively the systematics of E_{2^+} state in $^{114-130}$Xe. It may be noted from Table II that with the same calculational framework and without changing any parameter the observed shell closure at $N=82$ for ^{134}Te is exactly reproduced. We have also verified that with the present choice of the input parameters and the model of interaction the entire set of Sn isotopes turns out to be nearly spherical.

We next focus our attention on the factors that are responsible for making Xe isotopes to exhibit such features for 2_1^+ states. In Tables II and III, we present the results of occupation probabilities of various neutron and proton subshells for the ground states calculated from a HFB wave function generated for $^{114-130}$Xe isotopes.

A careful examination of proton occupation probabilities reveals that the four protons for the entire set of xenon isotopes are spread over nearly four states namely $3s_{1/2}$, $2d_{3/2}$, $2d_{5/2}$, and $1g_{7/2}$. Further, in the ^{122}Xe isotope, the $(2d_{3/2})_\nu$, and $(1g_{7/2})_\nu$ orbitals are nearly half filled, whereas $(1h_{11/2})_\nu$ orbital has about 4.95 neutrons. It is clear from these numbers that except for $k=5/2$ component of $(1h_{11/2})_\nu$ orbit, all the downsloping Nilsson orbits are fully occupied, resulting in giving rise to a maximum $\langle Q_0^2 \rangle$ moment and minimum value of the E_{2^+} energy for the ^{122}Xe nucleus. Thus, for the set of $^{114-122}$Xe nuclei, the systematic increase in the occupation probabilities of $(2d_{3/2})_\nu$, $(1g_{7/2})_\nu$, and $(1h_{11/2})_\nu$ orbits is responsible for the systematic increase of $\langle Q_0^2 \rangle$ moments and systematic decrease of

TABLE III. Subshell occupation numbers (protons) in the nuclei $^{114-130}$Xe and ^{134}Te.

Xenon nuclei (A)	Subshell occupation number						
	$3s_{1/2}$	$2d_{3/2}$	$2d_{5/2}$	$2f_{7/2}$	$1g_{7/2}$	$1h_{9/2}$	$1h_{11/2}$
^{114}Xe	0.55	0.93	1.98	0.00	0.46	0.00	0.08
^{116}Xe	0.56	1.03	1.72	0.00	0.61	0.00	0.07
^{118}Xe	0.57	1.07	1.57	0.00	0.71	0.00	0.07
^{120}Xe	0.57	1.07	1.54	0.00	0.73	0.00	0.07
^{122}Xe	0.59	1.11	1.52	0.00	0.83	0.00	0.06
^{124}Xe	0.58	1.09	1.55	0.00	0.76	0.00	0.02
^{126}Xe	0.57	1.08	1.67	0.00	0.69	0.00	0.02
^{128}Xe	0.56	1.02	1.73	0.00	0.60	0.00	0.08
^{130}Xe	0.55	0.99	1.84	0.00	0.54	0.00	0.06
^{134}Te	0.38	0.13	1.47	0.00	0.01	0.00	0.00

TABLE IV. Reduced transition probabilities for $E2$ transitions as well as the static quadrupole moments for the yrast levels in the nuclei $^{114-130}$Xe and ^{92,94}Zr. Here e_p (e_n) denote the effective charge for protons (neutrons). The empirical relations that $e_p = 1 + Z/A$ and $e_n = Z/A$ have been used for obtaining the numerical values for effective charges for Xe isotopes. For zirconium isotopes, we have used fixed values of effective charges. The entries presented in the third column correspond to the reduced matrix elements resulting from Eq. (15). The reduced matrix elements as well as the static moments have been expressed in a form that brings out their explicit dependence on the effective charges. The entries presented in the fifth and seventh columns correspond to the effective charges indicated in the first column. The $B(E2)$ values are in units of e^2 b^2 and static quadrupole moments have been given in units of e b.

Nucleus	Transition			$B(E2;J_i^+ \to J_f^+)$		$Q(J_f^+)$	
(e_p, e_n)	$(J_i^+ \to J_f^+)$	$[B(E2;J_i^+ \to J_f^+)]^{1/2}$	$[Q(J_f^+)]$	Theory	Expt.	Theory	Expt.
1	2	3	4	5	6	7	8
^{114}Xe							
	$0^+ \to 2^+$	$0.38e_p + 0.16e_n$	$-0.29e_p - 0.47e_n$				
	$2^+ \to 4^+$	$0.56e_p + 1.00e_n$	$-0.39e_p - 0.68e_n$				
	$4^+ \to 6^+$	$0.52e_p + 0.96e_n$	$-0.44e_p - 0.80e_n$				
	$6^+ \to 8^+$	$0.61e_p + 1.21e_n$	$-0.47e_p - 0.92e_n$				
	$8^+ \to 10^+$	$0.51e_p + 1.01e_n$	$-0.49e_p - 0.91e_n$				
^{116}Xe							
	$0^+ \to 2^+$	$0.48e_p + 0.86e_n$	$-0.30e_p - 0.55e_n$				
	$2^+ \to 4^+$	$0.57e_p + 1.04e_n$	$-0.39e_p - 0.70e_n$				
	$4^+ \to 6^+$	$0.59e_p + 1.10e_n$	$-0.43e_p - 0.78e_n$				
	$6^+ \to 8^+$	$0.29e_p + 0.60e_n$	$-0.47e_p - 0.99e_n$				
	$8^+ \to 10^+$	$0.64e_p + 1.45e_n$	$-0.49e_p - 1.10e_n$				
^{118}Xe							
(1.45,0.45)	$0^+ \to 2^+$	$0.49e_p + 1.05e_n$	$-0.31e_p - 0.67e_n$	1.40	1.38 ± 0.06[a]	-0.75	
	$2^+ \to 4^+$	$0.47e_p + 1.05e_n$	$-0.41e_p - 0.92e_n$				
	$4^+ \to 6^+$	$0.63e_p + 1.47e_n$	$-0.46e_p - 1.05e_n$				
	$6^+ \to 8^+$	$0.64e_p + 1.50e_n$	$-0.48e_p - 1.11e_n$				
	$8^+ \to 10^+$	$0.65e_p + 1.50e_n$	$-0.50e_p - 1.14e_n$				
^{120}Xe							
(1.45,0.45)	$0^+ \to 2^+$	$0.52e_p + 1.26e_n$	$-0.33e_p - 0.80e_n$	1.74	1.69 ± 0.09[a]	-0.84	
	$2^+ \to 4^+$	$0.39e_p + 0.90e_n$	$-0.41e_p - 0.96e_n$				
	$4^+ \to 6^+$	$0.61e_p + 1.38e_n$	$-0.44e_p - 0.99e_n$				
	$6^+ \to 8^+$	$0.62e_p + 1.40e_n$	$-0.46e_p - 1.04e_n$				
	$8^+ \to 10^+$	$0.63e_p + 1.40e_n$	$-0.48e_p - 1.07e_n$				
^{122}Xe							
(1.44,0.44)	$0^+ \to 2^+$	$0.51e_p + 1.27e_n$	$-0.33e_p - 0.81e_n$	1.67	1.42 ± 0.04[a]	-0.83	
	$2^+ \to 4^+$	$0.16e_p + 1.51e_n$	$-0.42e_p - 1.03e_n$				
	$4^+ \to 6^+$	$0.64e_p + 1.58e_n$	$-0.46e_p - 1.13e_n$				
	$6^+ \to 8^+$	$0.65e_p + 1.60e_n$	$-0.48e_p - 1.19e_n$				
	$8^+ \to 10^+$	$0.65e_p + 1.61e_n$	$-0.50e_p - 1.22e_n$				
^{124}Xe							
(1.43,0.43)	$0^+ \to 2^+$	$0.52e_p + 1.23e_n$	$-0.33e_p - 0.78e_n$	1.62	1.49 ± 0.09[b]	-0.81	
	$2^+ \to 4^+$	$0.62e_p + 1.47e_n$	$-0.42e_p - 1.00e_n$				
	$4^+ \to 6^+$	$0.65e_p + 1.53e_n$	$-0.46e_p - 1.09e_n$				
	$6^+ \to 8^+$	$0.64e_p + 1.51e_n$	$-0.49e_p - 1.13e_n$				
	$8^+ \to 10^+$	$0.62e_p + 1.45e_n$	$-0.50e_p - 1.12e_n$				
^{126}Xe							
(1.42,0.42)	$0^+ \to 2^+$	$0.46e_p + 0.97e_n$	$-0.33e_p - 0.70e_n$	1.12	0.77 ± 0.025[b]	-0.76	
	$2^+ \to 4^+$	$0.55e_p + 1.17e_n$	$-0.42e_p - 0.89e_n$				
	$4^+ \to 6^+$	$0.63e_p + 1.32e_n$	$-0.46e_p - 0.92e_n$				
	$6^+ \to 8^+$	$0.65e_p + 1.34e_n$	$-0.48e_p - 0.96e_n$				
	$8^+ \to 10^+$	$0.65e_p + 1.35e_n$	$-0.51e_p - 0.98e_n$				

TABLE IV. (*Continued.*)

Nucleus (e_p, e_n) 1	Transition $(J_i^+ \to J_f^+)$ 2	$[B(E2; J_i^+ \to J_f^+)]^{1/2}$ 3	$[Q(J_f^+)]$ 4	$B(E2; J_i^+ \to J_f^+)$ Theory 5	$B(E2; J_i^+ \to J_f^+)$ Expt. 6	$Q(J_f^+)$ Theory 7	$Q(J_f^+)$ Expt. 8
^{128}Xe							
(1.42,0.42)	$0^+ \to 2^+$	$0.50e_p + 0.92e_n$	$-0.32e_p - 0.58e_n$	1.20	0.75 ± 0.04[b]	-0.70	
	$2^+ \to 4^+$	$0.54e_p + 1.02e_n$	$-0.41e_p - 0.77e_n$				
	$4^+ \to 6^+$	$0.64e_p + 1.24e_n$	$-0.46e_p - 0.87e_n$				
	$6^+ \to 8^+$	$0.62e_p + 1.21e_n$	$-0.49e_p - 0.89e_n$				
	$8^+ \to 10^+$	$0.64e_p + 1.25e_n$	$-0.50e_p - 0.89e_n$				
^{130}Xe							
(1.41,0.41)							
	$0^+ \to 2^+$	$0.50e_p + 0.84e_n$	$-0.32e_p - 0.53e_n$	1.10	0.65 ± 0.05[b]	-0.67	
	$2^+ \to 4^+$	$0.60e_p + 1.00e_n$	$-0.41e_p - 0.67e_n$				
	$4^+ \to 6^+$	$0.62e_p + 1.04e_n$	$-0.45e_p - 0.73e_n$				
	$6^+ \to 8^+$	$0.64e_p + 1.06e_n$	$-0.49e_p - 0.76e_n$				
	$8^+ \to 10^+$	$0.64e_p + 1.06e_n$	$-0.51e_p - 0.77e_n$				
^{92}Zr							
(1.05,0.05)	$0^+ \to 2^+$	$0.25e_p + 0.44e_n$	$-0.16e_p - 0.28e_n$	0.081	0.083 ± 0.006[c]	-0.18	
	$2^+ \to 4^+$	$0.18e_p + 0.34e_n$	$-0.15e_p - 0.33e_n$	0.042	0.0177 ± 0.0004[c]	-0.17	
^{94}Zr							
(1.05,0.05)	$0^+ \to 2^+$	$0.27e_p + 0.60e_n$	$-0.17e_p - 0.38e_n$	0.098	0.066 ± 0.014[c]	-0.20	
	$2^+ \to 4^+$	$0.12e_p + 0.27e_n$	$-0.17e_p - 0.41e_n$	0.019	0.004[c]	-0.20	

[a]From Ref. [32].
[b]From Ref. [33].
[c]From Ref. [29].

E_{2^+} states. However, for the set of $^{124-130}$Xe nuclei, the above-mentioned orbits are more than half filled and then there is a tendency for the subshell closure of $(3s_{1/2})_\nu$ and $(2d_{5/2})_\nu$ for these nuclei.

B. Systematics of calculated values of $E2$ transition probabilities

In Table IV the calculated values of $E2$ transition probabilities between the states E_J and E_{J+2} are presented. The calculated values are expressed in parametric form in terms of the proton (e_p) and neutron (e_n) effective charges and have been obtained through a rigorous projection calculation. These two parameters have been chosen such that $e_p = 1 + e_{\text{eff}}$ and $e_n = e_{\text{eff}}$ so that only one parameter is introduced in the calculation. The $B(E2; J_i^+ \to J_f^+)$ values have been calculated in units of e^2 b^2. To have numerical values for these quantities, we have used the empirical relations for e_p and e_n as suggested by Mottelson [26,27]. He has shown that the effective charges resulting from the quadrupole polarization of the ''core'' are given by $e_p = [(A+Z)/A]e$ and $e_n = (Z/A)e$. The use of effective charges [28] is generally invoked in nuclear structure calculations to mock up the contribution made by the core towards the electromagnetic properties, due to its polarization as the nucleons are put in the valence space. The valence particles, through two-body effective interactions, can interact with the core and cause excitations. The calculated results indicate that by choosing $e_{\text{eff}} = Z/A$, a good agreement with the observed values for $B(E2; 0_1^+ \to 2_1^+)$ transition probabilities is obtained for the set of $^{118-124}$Xe nuclei. The calculated values of $B(E2; 0_1^+ \to 2_1^+)$ transition probabilities for the set of $^{126-130}$Xe isotopes are found to be larger as compared to their observed values. Besides this, our results on $B(E2)$ transition probabilities predict a very interesting feature. It has been found from our results that in the case of ^{116,124,128}Xe, $B(E2; 6_1^+ \to 8_1^+) < B(E2; 4_1^+ \to 6_1^+)$, which means that there is a slight dip in magnitude for $B(E2; 6_1^+ \to 8_1^+)$ values when compared to its neighbors. This dip is also predicted in ^{114}Xe and ^{120}Xe where it is found that $B(E2; 4_1^+ \to 6_1^+) < B(E2; 2_1^+ \to 4_1^+)$ and $B(E2; 2_1^+ \to 4_1^+) < B(E2; 0_1^+ \to 2_1^+)$, respectively. This feature is not obtained for the other isotopes. Further, if this dip is not found experimentally, it would constitute a serious discrepancy in our results, and in the case it is found experimentally, it would be an interesting confirmation of our calculations. On analyzing the experimental data, it has been found that Mach *et al.* [29] have experimentally measured the $B(E2)$ values for ^{92,94}Zr isotopes. The values presented by them in their paper clearly show a dip in $B(E2)$ values. For example, in ^{92}Zr, $B(E2; 0_1^+ \to 2_1^+)$ and $B(E2; 2_1^+ \to 4_1^+)$ values are 0.083(6) e^2 b^2 and 0.0177(4) e^2 b^2, respectively. In ^{94}Zr, $B(E2; 0_1^+ \to 2_1^+)$ and $B(E2; 2_1^+ \to 4_1^+)$ values are 0.066(14) e^2 b^2 and 0.004 e^2 b^2, respectively. We note that in both of these isotopes the $B(E2)$ values show a dip.

It therefore appears that ^{92,94}Zr could present ideal example for testing the theoretical approach that we have employed for the study of Xe isotopes. To this end, we have

carried out HFB and projection studies on ^{92,94}Zr nuclei using the same model for the two-body residual interaction. The values of the interaction parameters and the valence space employed are the same as in the earlier paper by Khosa *et al.* [20]. The results of these calculations for the $B(E2)$ values are presented at the end of Table IV and are seen to reproduce approximately the observed values for ^{92,94}Zr. As an illustration, the calculated and observed values for $B(E2)$ transition probabilities for the transitions $(0_1^+ \rightarrow 2_1^+ ; 2_1^+ \rightarrow 4_1^+)$ are (0.081 and 0.042 e^2 b^2) and [0.083(6) and 0.0177(4) e^2 b^2), respectively for ^{92}Zr. The low-lying yrast states in ^{92,94}Zr nuclei are also satisfactorily reproduced. The calculated and observed values of energies in MeV of $(0_1^+, 2_1^+, 4_1^+)$ states in ^{94}Zr are (0.0,0.69,1.38) and (0.0,0.91,1.47), respectively. In the case of ^{92}Zr, the corresponding values are (0.0,0.80,1.35) and (0.0,0.93,1.49), respectively. The comparison of calculated and observed results on ^{92,94}Zr thus establishes the validity of our theoretical approach. Therefore, if the dip is theoretically reproduced in ^{92,94}Zr isotopes, it would as well be happening in ^{114,116,120,124,128}Xe isotopes. This dip might be construed to imply structural change along the yrast states for ^{114,116,120,124,128}Xe isotopes.

C. Systematics of calculated values of Q_{J^+}

In Table IV the calculated values of Q_{J^+} are presented for the entire isotopic mass chain of xenon nuclei. These values are expressed in parametric form in terms of proton and neutron effective charges. We have calculated the $Q_{2_1^+}$ values for the same values of the effective charge as we have taken for the calculation of $B(E2; 0_1^+ \rightarrow 2_1^+)$ values. As a result of the nonavailability of the experimental Q_{J^+} values, it is not possible to make any comment regarding the degree of agreement with the observed values. In view of the quality of agreement for $B(E2; 0_1^+ \rightarrow 2_1^+)$ values, we are constrained to assume that the HFB wave function gives a reasonably good description of the xenon nuclei.

D. Yrast spectra

In Figs. 1(a) and 1(b), the low-lying yrast spectra of a chain of Xe isotopes are displayed. The low-lying yrast spectra are found to reproduce the experimental levels with $J^\pi \leqslant 6^+$ with reasonably acceptable discrepancy. The trend exhibited by the calculated 8_1^+ and 10_1^+ states in the nuclei ^{114,116,118}Xe is not consistent with the observed trend. It is true that the agreement for higher spins is poor. This is due to the fact that there is no free parameter in the energy calculation for the full isotopic mass chain $^{114-130}$Xe. This level of agreement can be considered to be nearly satisfactory because of a number of considerations. First, the calculation of yrast spectra is a complex many-body calculation involving a minimum of 14 valence particles for ^{114}Xe and a maximum of 30 valence particles for ^{130}Xe. Another noticeable fact is that the calculations are carried out for the entire set of Xe isotopes, with a single set of input parameters. The contribution of 4p-2h configuration to the energy of higher-lying states has not been calculated; nor we have used any parameter to simulate the contribution of the Sn core towards the moment of inertia. It was pointed out by Faessler [30] as well as by Praharaj [31] that doing so will provide further quantitative improvements in the calculated yrast spectra.

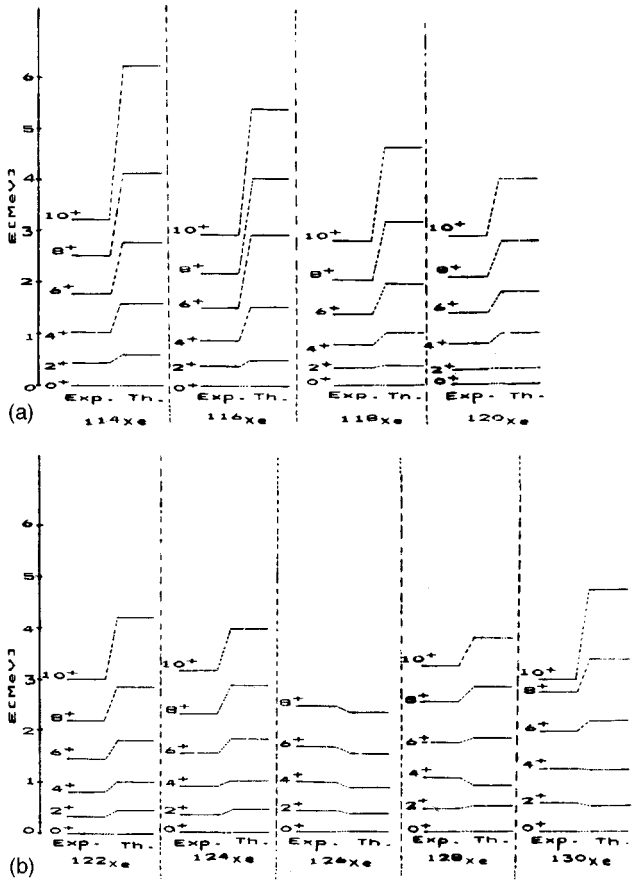

FIG. 1. (a) Experimental and theoretical low-lying yrast spectra for $^{114-120}$Xe nuclei (data taken from Refs. [34–37,43]). (b) Experimental and theoretical low-lying yrast spectra for $^{122-130}$Xe nuclei (data taken from Refs. [38–43]).

IV. CONCLUSIONS

To conclude it can be stated that the observed systematics of low-lying yrast spectra, $B(E2)$ transition probabilities, and Q_{J^+} values are found to get reproduced with a reasonable accuracy. Besides this, the results on $B(E2)$ transition probabilities in ^{114,116,120,124,128}Xe predict a slight dip which might be construed to imply different structures for ^{114,116,120,124,128}Xe as compared to their neighbours. It turns out that the VAP technique and quadrupole-quadrupole-plus-pairing model of interaction are fairly reliable for the calculation of yrast spectra in the entire set of xenon isotopes.

ACKNOWLEDGMENTS

We are grateful to Dr. G. K. Mehta, Dr. S. K. Dutta, and Dr. R. K. Bhowmik of Nuclear Science Centre, New Delhi, for making computational facilities available to perform VAP calculations of the present work. One of the authors (R.D.) is thankful to CSIR New Delhi for support.

[1] J. Genevey-Rivier, A. Charvet, G. Marguier, C. Richard Serre, J. D'Auria, A. Huck, G. Klotz, A. Knipper, and G. Walter, Nucl. Phys. **A238**, 45 (1977).
[2] E. W. Schneider, M. D. Glascock, W. B. Walters, and R. A. Meyer, Phys. Rev. C **19**, 1025 (1979).
[3] B. Singh, R. Iafigliola, K. Sofia, J. E. Crawford, and J. K. P. Lee, Phys. Rev. C **19**, 2409 (1979).
[4] C. Girit, W. D. Hamilton, and E. Michelakakis, J. Phys. G **6**, 1025 (1980).
[5] L. Goettig, Ch. Droste, A. Dygo, T. Morek, J. Srebrny, R. Broda, J. Styczen, J. Hattula, H. Helppi, and M. Jääskeläinen, Nucl. Phys. **A357**, 109 (1981).
[6] W. Gast, U. Kaup, H. Hanevinkel, R. Reinhardt, K. Schiffer, K. P. Schmittgen, K. O. Zell, J. Wrzesinski, A. Gelberg, and P. V. Brentano, Z. Phys. A **318**, 123 (1984).
[7] R. Reinhardt, A. Dewald, A. Gelberg, W. Lieberz, K. Schiffer, K. P. Schmittgen, K. O. Zell, and P. Von Brentano, Z. Phys. A **329**, 507 (1988).
[8] Dan Jerrestam, S. Elfström, W. Klamra, Th. Lindblad, C. G. Lindèn, V. Barci, H. El-Samman, and J. Gizon, Nucl. Phys. **A481**, 355 (1988).
[9] P. F. Mantica Jr., B. E. Zimmerrman, W. B. Walters, J. Rikovska, and N. J. Stone, Phys. Rev. C **45**, 1586 (1992).
[10] S. G. Rohozinski, J. Dobaczewski, B. Nerlo Pomorska, K. Pomorski, and J. Srebrny, Nucl. Phys. **A292**, 66 (1977); Report No. IFT/77/7, Warsaw, 1977; Report No. IFT/77/8, Warsaw, 1977.
[11] T. Otsuka, A. Arima, F. Lachello, and I. Talmi, Phys. Lett. **76B**, 139 (1978); T. Otsuka, A. Arima, and F. Lanchello, Nucl. Phys. **A309**, 1 (1978).
[12] N. Onishi and S. Yoshida, Nucl. Phys. **80**, 367 (1966).
[13] M. Baranger, Phys. Rev. **130**, 1244 (1963).
[14] J. D. Vergados and T. T. S. Kuo, Phys. Lett. **35B**, 93 (1971).
[15] P. Federman, S. Pittel, and R. Comos, Phys. Lett. **82B**, 9 (1979).
[16] M. K. Pal, *Theory of Nuclear Structure* (Affiliated East-West Press, New Delhi, 1982).
[17] T. Engeland, M. Hjorth-Jensen, A. Holt, and E. Osnes, Phys. Rev. C **48**, R535 (1993).
[18] M. Baranger and K. Kumar, Nucl. Phys. **A110**, 490 (1968).
[19] A. Arima, Nucl. Phys. **A354**, 19 (1981).
[20] S. K. Khosa, P. N. Tripathi, and S. K. Sharma, Phys. Lett. **119B**, 257 (1982).
[21] K. Kumar *et al.*, Phys. Rev. C **16**, 1235 (1977).
[22] A. Faessler, L. Lin, and F. Wittman, Phys. Lett. **44B**, 127 (1973).
[23] S. C. K. Nair and A. Ansari, Phys. Lett. **47B**, 200 (1973).
[24] S. Das Gupta and A. Van Ginneken, Phys. Rev. **164**, 1320 (1967).
[25] L. Grodzins, Phys. Lett. **2**, 88 (1962).
[26] B. R. Mottelson, in *Many Body Problem*, edited by C. DeWitt (New York, Wiley, 1959), p. 289.
[27] A. Bohr and B. R. Mottelson, *Nuclear Structure* (Benjamin, Reading, MA, 1975), Vol. II, p. 515, and Vol. I.
[28] P. N. Tripathi and S. K. Sharma, Phys. Rev. C **34**, 1081 (1986).
[29] H. Mach, E. K. Warburton, W. Krips, R. L. Gill, and M. Moszynski, Phys. Rev. C **42**, 568 (1990).
[30] A. Faessler, in *Proceedings of the Conference on High Angular Momentum Properties of Nuclei*, Oak Ridge, 1982, edited by N. R. Johnson (Harwood Academic, Chur, Switzerland, 1983).
[31] C. R. Praharaj, Phys. Lett. **119B**, 17 (1982).
[32] S. Raman, J. A. Sheikh, and K. H. Bhatt, Phys. Rev. C **52**, 1380 (1995).
[33] S. Raman, C. H. Malarkey, W. T. Milner, C. W. Nestor Jr., and P. H. Stelson, At. Data Nucl. Data Tables **36**, 22 (1987).
[34] J. Blachot and G. Marguier, Nucl. Data Sheets **474**, 821 (1995).
[35] J. Blachot and G. Marguier, Nucl. Data Sheets **73**, 203 (1994).
[36] K. Kitao, Nucl. Data Sheets **75**, 186 (1995).
[37] A. Hashizume, Y. Tendow, and M. Ohshima, Nucl. Data Sheets **52**, 645 (1987).
[38] T. Tamura, Nucl. Data Sheets **71**, 534 (1994).
[39] T. Tamura, K. Miyano, and S. Ohya, Nucl. Data Sheets **41**, 415 (1984).
[40] T. Tamura, K. Miyano, and S. Ohya, Nucl. Data Sheets **36**, 243 (1982).
[41] K. Kitao, M. Kanbe, and Z. Matumoto, Nucl. Data Sheets **38**, 210 (1983).
[42] Yu. V. Sergeenkov, Nucl. Data Sheets **58**, 785 (1989).
[43] M. Sakai, At. Data Nucl. Data Tables **31**, 399 (1984).